A novel RGD-independent cell adhesion pathway mediated by fibronectin-bound tissue transglutaminase rescues cells from anoikis

Elisabetta A.M. Verderio[*], Dilek Telci[*], Afam Okoye[*], Gerry Melino[§] and Martin Griffin[*|]

[*] Dept. of Life Sciences, Nottingham Trent University, Clifton Lane, Nottingham, UK; [§]IDI-IRCCS, c/o Dept. of Experimental Medicine, D26/F153, University of Rome "Tor Vergata", Rome, Italy.

[|]Corresponding author: M Griffin, Department of Life Sciences, Nottingham Trent University, Clifton Lane, Nottingham, NG11 8NS, UK. Tel.: +44 (0) 115 848 6670. Fax: +44 (0) 115 848 6636. Email: martin.griffin@ntu.ac.uk.

Key words: transglutaminase; fibronectin; proteoglycans; anoikis; repair

Running title:

RGD-independent cell adhesion by tissue transglutaminase-fibronectin complex.

SUMMARY

Specific association of tissue transglutaminase (tTG) with matrix fibronectin results in the formation of an extracellular complex (tTG-FN) with distinct adhesive and pro-survival characteristics. tTG-FN supports RGD-independent cell adhesion of different cell types and the formation of distinctive RhoA-dependent focal adhesions following inhibition of integrin function by competitive RGD peptides and function blocking anti-integrin antibodies $\alpha_5\beta_1$. Association of tTG with its binding site on the 70 kda amino-terminal FN fragment does not support this cell adhesion process, which seems to involve the entire FN molecule. RGD-independent cell adhesion to tTG-FN does not require transamidating activity, is mediated by the binding of tTG to cell-surface heparan sulfate chains, is dependent on the function of protein kinase Cα (PKCα) and leads to activation of the cell survival focal adhesion kinase (FAK). The tTG-FN complex can maintain cell viability of tTG-null mouse dermal fibroblasts when apoptosis is induced by inhibition of RGD-dependent adhesion (anoikis), suggesting an extracellular survival role for tTG. We propose a novel RGD-independent cell adhesion mechanism that promotes cell survival when the anti-apoptotic role mediated by RGD-dependent integrin function is reduced as in tissue injury, which is consistent with the externalisation and binding of tTG to fibronectin following cell damage/stress.

INTRODUCTION

Subtle changes in the extracellular matrix (ECM) complexity/tissue architecture may be crucial for the regulation of the apoptotic machinery leading to anoikis (1, 2). Such a process occurs during tissue injury when the composition and integrity of the ECM are altered in several significant ways (3). A central component of the ECM, which regulates adhesion-dependent survival signalling, is the adhesive glycoprotein fibronectin (FN) (4). FN binds to cell-surface matrix receptors, primarily the $\alpha_5\beta_1$ integrins, through the ArgGlyAsp (RGD) cell-binding site within the Type III_{10} domain. The importance of the RGD cell binding domain in adhesion-mediated cell survival has been demonstrated by employing synthetic peptides containing the RGD motif, which induce apoptosis in many cell types, by acting as competitive inhibitors of FN-integrin interaction and activators of caspase 3 (5, 6). A comparable scenario may occur in wounding and inflammatory conditions, whereby fragmentation of FN, can lead to detachment-induced apoptosis (7, 5). However, the RGD cell-binding domain of FN is not sufficient in isolation to regulate cell survival, which must be sustained by other critical FN domains such as the C-terminal heparin binding domain (HepII) (7, 8), known to synergistically interact with heparan sulfate proteoglycans (HSPG) receptors and integrin $\alpha_4\beta_1$ (9). Evidence is also accumulating to suggest that changes in the molecular structure and composition of the FN matrix may provide new signals to regulate cell shape, migration and proliferation. Alterations to the conformation of FN either by multimerization (10) or heterotypic association with other matrix molecules (11) could reveal biologically active neo-epitopes, which regulate cell responses via the induction of cytoskeleton assembly (12). Modulation of the FN matrix may therefore also be fundamental in the regulation of adhesion-related apoptosis.

One protein which binds with high affinity specialised FN domains and modulates the function of FN is tissue-type transglutaminase (tTG, TG-2) (13, 10, 14). tTG is a multifunctional protein implicated in diverse normal and pathological processes (15) but more specifically is regarded as an important component of cell/tissue defence in response to cell damage and stress (16, 17). tTG differs from the other transglutaminases in that the transamidase active site is integrated with a GTP binding/hydrolysis site,

which negatively regulates the transamidation activity by structurally blocking the active site (18). Another peculiarity of tTG is its externalisation into the ECM via a non Golgi/ER route, through a mechanism which appears to depend on its active-state conformation (19) and an intact FN binding site in the 28 kd amino-terminal sandwich region (20, 21). Matrix deposition of tTG increases in situations of tissue damage and cellular stress and results in the immobilisation of tTG on matrix FN (16, 17, 22, 20), which in turn protects tTG from matrix degradation (23). Consistent with these findings is the observation that guinea pig liver tTG forms specific complexes with human plasma FN and it appears as a globular protein bound to the N-terminal portion of FN interacting either with the Type I_4-I_5 motif (24) or with a sequence within the gelatin-binding domain of FN (I_6-II_1-II_2-I_7-I_8-I_9) (13).

The involvement of tTG in the adhesion of multiple cell types is now consolidated (25, 26), however the molecular mechanism and its physiological significance remain controversial. It has been proposed that tTG enhances cell adhesion through matrix remodelling, via protein crosslinking (10, 26), however recent findings suggest that tTG involvement in cell-matrix interactions is independent from its transamidation activity (27, 28, 19). Cell-surface tTG might act as an adhesion co-receptor of integrins β_1 and β_3 by mediating cell adhesion to the gelatin binding domain of FN (27) or, conversely, act as an independent adhesion protein, by specific binding to $\alpha_4\beta_1$ and $\alpha_9\beta_1$ integrins (28).

In the current study we have explored the involvement of tTG in FN-mediated cell survival, starting with the hypothesis that the ECM function of tTG is strictly dependent on its association with FN, and that tTG and FN reciprocally modulate each others functions following complex formation. We report that FN-bound tTG supports a novel RGD-independent cell adhesion process, which is mediated by the direct binding of tTG to the cell surface through a mechanism that is critically dependent on cell-surface heparan sulfate and activation of protein kinase Cα (PKCα). We describe that FN-bound tTG, but not FN can rescue tTG-deficient mouse dermal fibroblasts from apoptosis induced by inhibition of RGD-dependent cell adhesion (anoikis), with maintenance of cell viability. Our findings suggest that matrix FN with bound tTG is functionally distinct from either protein acting in isolation and suggest a novel RGD-independent pathway which may be important in cell survival under conditions of cell damage/stress.

EXPERIMENTAL PROCEDURES

Reagents and antibodies

Mouse monoclonal antibodies included anti-integrin β_1 (JB1A) and α_5 (PID6) (Chemicon), vinculin, tubulin (Sigma-Aldrich), tTG (Cub74) (NeoMarkers). Rabbit polyclonal antibodies included anti-human fibronectin (Sigma-Aldrich) and anti-human phospho(Tyr397)-FAK (Upstate Biotechnology). The tTG inhibitor R283 (19) was synthesised by R. Saint and I. Coutts, Nottingham Trent University. Purified guinea pig liver tTG was either obtained by Sigma-Aldrich or purified according to Leblanc et al (1999) (29). Human plasma FN and FN proteolytic fragments, GTPγ-S, and synthetic RGD specific peptides (GRGDTP and GRGDSP) were from Sigma-Aldrich, control RAD peptide (GRADSP) from Calbiochem. Heparitinase (EC4.2.2.8) was from Sigma-Aldrich, and chondroitinaseABC (protease-free) from Seikagaku Corporation. The PKCα inhibitor GO6976 was from Calbiochem.

Cell lines

Primary human osteoblasts (HOB) were provided by S. Downes (University of Nottingham, UK) and maintained in Dulbecco's modified Eagle's medium (DMEM) as we previously described (30). Swiss 3T3 albino fibroblasts were obtained from American Type Culture Collection and maintained in DMEM supplemented with 10%(v/v) foetal calf serum (FCS), 2 mM glutamine, and penicillin/streptomycin (100 U/ml and 100 μg/ml, respectively). Transfected Swiss 3T3 fibroblasts, displaying inducible expression of tTG (clone TG3), were cultured and induced as described by Verderio et al (1998), (22). Primary mouse dermal fibroblasts (MDF) were isolated from the skin of tTG-deficient (MDF-TG-/-) and wild type (MDF-TG+/+) 9-months old mice and maintained as described by De Laurenzi and Melino (2001), (31).

Immobilisation of TG on FN and amino-terminal FN fragments

96-well plates were coated with human plasma FN (5 μg/ml) or with the 70 kd (42 μg/ml), 45 kd (54 μg/ml), and 30 kd (54 μg/ml) proteolytic fragments of FN in 50 mM Tris-HCl, pH 7.4, 50 μl/well, by incubation at 4 °C for approximately 15 h.

Concentrations of FN and FN fragments were optimal to saturate tissue culture plastic (TCP), as measured by an ELISA-based assay with polyclonal anti-FN antibody (1/5000) followed by peroxidase-labelled anti-rabbit IgG (1/5000). FN fragments were in a 30-, 60- and 90-fold stoichiometric excess, respectively, of control FN. For tTG immobilisation, the FN solution was removed, the wells were washed once in 50 mM Tris-HCl, pH 7.4, and then incubated with purified guinea pig liver tTG (20 μg/ml) in phosphate-buffered saline (PBS) containing 2 mM EDTA , 100 μl/well. After 1 h at 37 °C, the tTG solution was removed and wells were washed once in 50 mM Tris-HCl, pH 7.4, and once in serum-free culture medium before cell seeding. In some experiments FN coated plates were blocked with 3%(w/v) lipid milk protein (Marvel) in PBS at 37 °C for 30 min and then washed twice with 50 mM Tris-HC1, pH 7.4, prior to tTG immobilisation. The presence of tTG immobilised on FN was confirmed by an ELISA-type assay using Cub74 as we previously described (26). The transamidating activity of the immobilised tTG was determined by the incorporation of biotinylated cadaverine into FN as previously described (26) and compared with the activity of free tTG standard. Data are expressed as absorbance 450nm with 5 mM Ca^{2+} in the reaction buffer minus background absorbance values with 5 mM EDTA.

Cell adhesion assay

Exponentially growing cells were detached using 0.25%(w/v) trypsin in 5 mM EDTA, collected into medium containing a ~7%(v/v) FCS, washed twice with medium without FCS and then plated onto 96-well plates (2×10^4 cells/well), coated with FN or FN fragments, with and without immobilised tTG. After a maximum of 20 min incubation (to minimise the secretion of any endogenous protein) at 37 °C in a 5% CO2 atmosphere, cells were fixed in 3.7%(w/v) paraformaldehyde (PFM) in PBS, permeabilised in 0.1%(v/v) Triton X-100 in PBS and stained with May Grunwald and Giemsa stain (26). In some cases cells were pre-treated for 15 h with 1 mM cycloheximide before plating, to rule out any effects of endogenous secreted adhesion molecules. Digital images of 3 non-overlapping fields covering the central portion of each well were captured using a video digital camera (Olympus DP10) and examined using the Image Analysis programme Scion Image (National Institute of Health, USA). At least 9 images of separate fields per

sample were examined for a total of at least 400 cells in the FN control. The number of attached cell particles in each field was measured by "thresholding" and "particle analysis" and the spread cells by "density slicing".

Cytoskeletal staining

Actin stress fibres were visualised using fluorescein isothiocyanate (FITC)-labelled phalloidin and focal adhesions by staining for vinculin. Cells were seeded in 0.79 cm^2 wells of chamber slides (8×10^4 cells /well) previously coated with FN and tTG-FN and allowed to adhere for ~20 min. Cells were fixed using 3.7%(w/v) PFM in PBS and permeabilised in 0.1%(v/v) TritonX-100 in PBS. For actin stress fibres, cells were then blocked in PBS buffer supplemented with 5%(w/v) dry milk and then incubated with FITC-labelled phalloidin (20 μg/ml) in blocking buffer. For localisation of vinculin, cells were blocked in PBS buffer containing 3%(w/v) bovine serum albumin (BSA) and then incubated with mouse monoclonal anti-vinculin antibody (1:100) in blocking buffer. Bound antibody was revealed by incubation with rabbit anti-mouse IgG-FITC (1:100) (Dako) in blocking buffer. Coverslips were mounted with Vectashield mountant containing propidium iodide (Vector Laboratories) and examined by laser confocal microscopy using a Leica TCSNT system (Leica Lasertechnik). Consecutive scanning sections (~2 μm) from the upper to the bottom attachment site of cells were overlaid as an extended focus image and imaged cells (from at least 8 random fields, at least 100 cells in FN control) were scored for actin stress fiber formation with the aid of the Leica TCSNT (version 1.5-451) image processing menu.

Inhibition of integrin-mediated cell adhesion

Cells in suspension (2×10^5 cells/ml) were incubated with GRGDTP synthetic peptide (32) (50 μg/ml, ~75 μM, 100 μg/ml ~150 μM, or 200 μg/ml ~300 μM). Some experiments were reproduced using the FN-prototype GRGDSP peptide. Alternatively, cells in suspension (2×10^5 cells/ml) were incubated with function blocking anti-integrin antibodies (JB1A, 40 μg/ml and P1D6, 30 μg/ml). All incubations were performed in serum-free medium at 37 °C for 10 min after that cells were seeded in the presence of either the competitive RGD peptides or the anti-integrin antibodies.

Cell treatment with C3 exotranferase

Clostridium botulinum C3 exotransferase (Biomol) (20 μg/ml) was incubated with lipofectamine (100 μg/ml) (Life Technologies) in DMEM at 22 °C for 1 h after that the complex was diluted 10 times in DMEM and added to duplicate 18-h old cell monolayers (~80% confluent) in serum-free medium. After 2 h the medium was removed, cells allowed to recover for ~30 min in serum-containing DMEM and then seeded in 0.79 cm^2-wells of chamber slides (45×10^3 cells/well).

Quantification of anoikis and measurement of cell viability

For fluorochrome labelling of DNA strand breaks, 6×10^5 cells were seeded in duplicate in 9.6 cm^2-wells pre-coated with FN or tTG-FN in the presence or absence of RGD peptide. After 15 h incubation at 37 °C in a 5% CO2 atmosphere, all cells (adhered and nonadhered) were collected, washed twice in PBS , resuspended at the final concentration of 1.2×10^7 cells/ml and fixed in suspension by addition of one volume of 4%(w/v) PFM in PBS. Cells were then permeabilised in 0.1%(v/v)TritonX-100 in 0.1%(w/v) sodium citrate buffer, for 2 min on ice (to minimise loss of fragmented DNA). Cells were labelled with terminal deoxynucleotidyl transferase (TdT) and FITC-dUTP, using a TUNEL kit according to the manufacturer (Roche). The fluorescence intensity was measured by flow cytometry using a Beckman Coulter EPICS XL. Cells were collected and data stored and analysed using the software SYSTEM II and WinMDI2.8. DNA fragmentation was also detected by *in situ* analysis of nuclei following TUNEL, by confocal fluorescent microscopy. Cells found in suspension were fixed and labelled in triplicate on 0.79 cm^2-wells of glass slides (~5 $x10^4$ cells/well). For quantification, the Leica LCS software was used to acquire 3 random images per well for a total of 9 images per experimental sample using a fixed protocol (with constant photo-multiplier tube and section-depth setting). Data are expressed as mean number of apoptotic cells per well. Cell viability was assessed by a colorimetric assay based on the metabolism of the tetrazolium salt XTT (Roche), after an incubation period of 4 h with XTT. Data are expressed as absorbance values at 492nm after subtraction of values at 690nm.

Statistics

Data are expressed as mean ±SD and represent one of at least 3 separate experiments undertaken in triplicate, unless stated otherwise. Differences between data sets were determined by the Student's t-test (two-tailed distribution, two-sample equal variance). Differences described as significant in the text correspond to $p<0.05$.

RESULTS

Tissue transglutaminase bound to FN supports RGD independent-cell adhesion of different cell types

Previous work using fluorescent microscopy and immunogold electron microscopy demonstrated a close association of tTG with FN at the cell surface/pericellular matrix (22, 20), consistent with the *in vitro* specific binding of the enzyme with human plasma FN (24, 13). To investigate how tTG in complex with FN affects FN cell adhesion, we first bound purified guinea pig liver tTG to human plasma FN coated onto tissue culture plastic (TCP). EDTA was included in the reaction to inhibit tTG transamidating activity. Measurement of binding by an ELISA-type assay showed that FN, immobilised at the saturating concentration of 5 μg/ml, bound a saturating amount of tTG when incubated with 20 μg/ml free tTG (Fig. 1 A). Using this initial matrix model of immobilised FN with bound tTG (tTG-FN), the contribution tTG to FN cell adhesion was examined by inhibiting integrin-mediated RGD-dependent cell adhesion with competitive concentrations of soluble RGD peptides. Human osteoblast-like cells (HOB) were selected as the initial cell model since they preferentially adhere on FN *in vitro*, demonstrate an enhanced spread morphology on biomaterials coated with tTG-FN (33) and are characterised by a well defined pattern of integrin cell-surface receptors, consisting mainly of RGD-binding β1 subunit paired with α_1, α_2, α_3, α_5 and α_V subunits (34). In the absence of RGD peptide, attachment to tTG-FN was comparable to FN (Fig. 1 B, upper), although cell spreading appeared to be enhanced on tTG-FN (Fig. 1 B, lower). At 50 and 100 μg/ml RGD peptide, attachment on FN was significantly reduced (typically to 30-50% of control values on FN) (Fig. 1 B, upper), but attachment to tTG-FN was not significantly inhibited at these same RGD peptide concentrations. Cell attachment to tTG-FN in the presence of 100 μg/ml RGD peptide was 85-95% of control cell attachment to FN without RGD peptide. Only at 200 μg/ml, was cell attachment to tTG-FN significantly lower in comparison to control FN without RGD peptide. At this higher concentration, the RGD peptide may in part act non-specifically, since the control RAD peptide also led to a small reduction in cell attachment at 200 μg/ml (Fig. 1 B, upper inset). Incubation of cells with RGD peptide, significantly reduced cell spreading

on FN (Fig. 1 B, lower), typically to 10-50% of control value at 100 μg/ml RGD peptide, but as for cell attachment, cell spreading was only partially reduced on tTG-FN at 50 and 100 μg/ml RGD peptide (usually to 65-85% of control values on FN). Swiss 3T3 fibroblasts displayed a comparable response to HOB cells on the tTG-FN complex. Attachment (Fig. 1 C upper) and spreading (Fig. 1 C, lower) of Swiss 3T3 fibroblasts to FN was significantly decreased with excess RGD peptide, in a more sensitive way than in osteoblasts (typically to 25-35% of control at 100 μg/ml RGD peptide), but was restored to control levels when cells were seeded onto tTG-FN at 50 and 100 μg/ml RGD peptide. An epithelial-like cell line (ECV304) also adhered more efficiently on tTG-FN than FN in the presence of excess RGD peptide (Fig. Suppl. 1). When cells were seeded onto TCP coated with tTG without prior immobilisation of FN, cell attachment was found to be negligible at concentrations ranging from 20 to 50 μg/ml of tTG, in the absence or presence of competitive RGD peptide (Fig. 1 C). Plates were coated with saturating amounts of FN and blocking of FN-coated wells with 3% non-fat milk protein prior to tTG immobilisation did not affect RGD-independent cell attachment and spreading supported by the tTG-FN matrix formed in the absence of blocking (data not shown). These findings clearly indicate that the complex of tTG bound to FN is the essential component for the RGD-independent cell adhesion to occur. Association of purified tTG to free human plasma FN in solution prior to immobilisation onto TCP, with the suggested stoichiometry of approximately 2:1 (24), also led to a matrix able to significantly support RGD-independent cell adhesion and spreading (which respectively were 80±1.4 and 98±3.9 of control FN, in a typical experiment with 100 μg/ml RGD peptide). Cells pre-treated with cycloheximide, to rule out secretion of endogenous adhesion molecules, were still capable of RGD-independent cell attachment on tTG-FN (data not shown). Together these data show that binding of tTG to FN supports a novel RGD-independent pathway.

tTG immobilisation on amino-terminal FN fragments is not sufficient to mediate RGD-independent adhesion of osteoblast-like cells

Since tTG is known to bind to FN at a domain within the 70 kd amino-terminal fragment (24, 13) we explored whether association of tTG to N-terminal FN peptides was

sufficient to support RGD-independent cell adhesion. tTG was immobilised on the 70 kd (matrix assembly, heparin and gelatin binding), 45 kd (gelatin-binding) and 30 kd (first type I repeats, matrix assembly, heparin binding) amino-terminal FN peptides. Detection of the relative levels of tTG by ELISA showed that incubation of the FN fragments with 20 μg/ml tTG resulted in saturating levels of tTG immobilised on all fragments (Fig. 2 A). Cell adhesion of HOB cells to the different FN fragments alone or in complex with tTG was compared. On the 70 kd fragment alone, both cell attachment and spreading in the absence of RGD peptide were ~80% the values obtained on FN (Fig. 2 B upper and lower, respectively), however on the 45 kd and 30 kd fragments cell attachment and cell spreading were only ~10% and ~5% of control FN, respectively. In the presence of RGD peptide, cell attachment and spreading values on the 70 kd fragment were significantly inhibited by ~40% (Fig. 2 B upper and lower, respectively). This data agrees with previous findings that the amino-terminal of FN binds the integrin $\alpha_5\beta_1$ in cross-competition with the RGD peptide (Hocking et al 2000). Immobilisation of tTG on the 70 kd fragment unlike FN did not induce RGD-independent cell attachment and spreading but led to further deterioration of cell adhesion (Fig. 2 B). Yet tTG did not enhance cell adhesion to the 70 kd fragment even in the absence of the RGD peptide. Furthermore, tTG did not improve cell adhesion on the 45 kd and 30 kd fragments, which remained at negligible levels (Fig. 2 B). These results indicate that adhesion of HOB cells to the amino-terminal 45 kd and 30 kd FN fragments, which contain putative tTG binding sites (13, 24), is negligible regardless of the binding of tTG and that tTG binding to the 70 kd peptide is not sufficient to sustain RGD-independent cell adhesion.

RGD-independent cell adhesion to FN with immobilised tTG promotes formation of unique focal adhesion structures

Formation of actin stress fibers in the presence of integrin-binding RGD peptide in response to tTG-FN was analysed by confocal laser scanning microscopy utilizing FITC-phalloidin. HOB cells adhered to FN did not show organised stress fibers following RGD peptide treatment (Fig. 3 A, c), compared to non-treated cells (Fig. 3 A, a), which exhibited a flat morphology and extensive actin stress fibers. In contrast, most of the cells seeded on tTG-FN were spread and had organised actin stress fibers despite the RGD

peptide (Fig. 3 A, d), however the actin fibers formed were shorter and less organised than those assembled in control cells adhered to FN in the absence of RGD peptide (Fig. 3 A, a). Without RGD peptide, actin stress fibres appeared more dense and well-formed in response to tTG-FN than FN (Fig. 3 A, b and a, respectively), confirming that immobilised tTG enhances cell spreading (see Fig. 1 B). Staining for vinculin indicated the absence of punctate characteristic focal contacts of FN-adhered cells (Fig. 3 A, e) in the RGD-treated cells adhered to FN (Fig. 3 A, g) but not in those adhered to tTG-FN (Fig. 3 A, h). Relative measurement of the formed actin stress fibres (Fig. 3 A, graph) confirmed that the RGD peptide did not affect the formation of focal adhesions in cells plated on tTG-FN, although it significantly affected the quality of the actin reorganisation, as shown by fluorescence microscopy (Fig. 3 A, d). Treatment of cells with the function blocking anti-integrin β_1 (JBIA) and, to a lesser extent α_5 antibody (PID6), led to a large decrease of actin stress fibers on FN (Fig. 3 B, b and c, respectively), compared to cells incubated with non-specific IgG (Fig. 3 B, a). In contrast, on tTG-FN, cells incubated with the anti-integrin antibodies appeared to maintain a network of actin stress fibers (Fig. 3 B, e and f), although less elaborated and dense than in control cells treated with IgGs (Fig. 3 B, d). Comparison of the number of formed actin stress fibers (Fig. 3 B, graph) statistically confirmed these observations that tTG-FN leads to the formation of integrin β_1 and α_5 independent actin filaments even though more rudimental than in the absence of inhibition. RGD-independent adhesion of cells to tTG-FN was dependent on GTPase RhoA, since inhibition of RhoA activity by botulinum toxin C3 exotransferase almost completely blocked RGD-independent assembly of actin stress fibers in response to tTG-FN (Fig. 3 C).

tTG cross-linking activity is not required to support RGD-independent cell adhesion

We next assayed the transamidating activity of FN-bound tTG to establish its potential role in the described RGD independent cell adhesion process. The activity of tTG once bound to FN was negligible when measured in cell culture medium DMEM, which contains an activating concentration of Ca^{2+} (1.9 mM), and was not changed by addition of further Ca^{2+}, but was significantly boosted by pre-incubation of tTG with DTT prior to immobilisation on FN (Fig. 4 A), as described (26). Hence, under the conditions used

FN-bound tTG is not active in the presence of cell culture medium, unless its cysteine residues, particularly the active-site Cys_{277}, are kept in a reduced state. The transamidation-independent role of tTG in the RGD-independent cell adhesion process was further confirmed by utilizing the irreversible inhibitor R283, a 2-[(2-oxopropyl)thio]imidazolium derivative (19). HOB cells were incubated with R283 and plated on a tTG-FN matrix pre-treated with R283, in the absence or presence of RGD peptide. Under these conditions the activity of the immobilised tTG, is completely blocked by the inhibitor (Fig. 4 C). The low tTG activity found at the HOB cell surface (30) is also inhibited to negligible values by equal concentrations of R283 (unpublished data). Cell adhesion on FN bound to inactivated tTG was not significantly different to cell adhesion on FN bound to tTG not treated with the inhibitor, with or without pre-treatment of cells with RGD peptide, and it was typically twice cell adhesion on FN in the presence of RGD peptide (Fig. 4 B; cell attachment, upper and cell spreading, lower). These data clearly indicate that FN-bound tTG does not require its transamidating activity to promote RGD-independent cell adhesion.

Evidence for the importance of FN-associated tTG and its calcium-induced conformation in cell-surface recognition

To assess the importance of tTG in cell-surface interaction, FN-bound tTG was blocked by using the monoclonal anti-tTG antibody Cub74, in conditions that fully preserved the availability of FN in this complex. This was demonstrated by the unchanged recognition of FN by anti-FN polyclonal antibody after treatment of tTG-FN with either Cub74 or control IgG (Fig. 5 B). Obstruction of tTG by Cub74 completely abolished the RGD-independent cell adhesion mediated by tTG-FN (Fig. 5 A; cell attachment, upper and cell spreading, lower), suggesting a direct role for FN-associated tTG in the RGD-independent binding to cells. tTG can assume two conformations, depending on whether it is bound to GTP/GDP or Ca^{2+} (18). In the extracellular environment, tTG is likely to assume the Ca^{2+}-induced open structure. Incubation of FN-bound tTG with the non hydrolysable GTP-γS (1 mM), significantly reduced the RGD-independent cell attachment and spreading mediated by tTG-FN (Fig. 5 C, upper and lower, respectively). Since incubation of tTG with GTP-γS did not significantly alter the level of tTG bound to

FN (Fig. 5 D), our results suggest that RGD-independent cell adhesion to tTG-FN critically depends on the calcium-mediated tertiary structure of tTG.

Role of cell-surface heparan sulfate in RGD-independent cell adhesion and signalling via tTG-FN

To explore the possibility that cell adhesion to tTG-FN may be mediated by a cell-surface proteoglycan, HOB cells were treated with glysosaminoglycan-degrading enzymes. Degradation of cell-surface heparan sulfate chains with heparitinase (15 mU/ml) led to a reduced cell attachment to FN (~70% of control values) (Fig. 6 A, upper), as expected given the importance of cell-membrane heparan sulfate proteoglycans (HSPG) in the adhesion of osteoblast-like cells (34). It also led to complete abolishment of RGD-independent cell attachment and spreading on tTG-FN (Fig. 6 A, upper and lower respectively). In contrast, equal concentrations of protease-free chondroitinase ABC had no significant effect on cell adhesion to FN, did not significantly alter RGD-independent cell spreading on tTG-FN (Fig. 6 A, lower) and only marginally affected cell attachment (Fig. 6 A, upper). These results demonstrate that RGD-independent cell adhesion to tTG-FN critically depends on cell-surface heparan sulfate and suggest the involvement of cell-surface heparan sulfate proteoglycans (HSPG) and not chondroitin sulfate proteoglycans in this process. Syndecan-4 is the only known HSPG that is a widespread component of focal adhesions and downstream signalling specifically involves PKCα (35). Cells were therefore treated with the selective PKCα inhibitor G06976 (36) prior to and during the cell adhesion experiments. Following G06976 incubation, a significant inhibition (~30%) of both attachment and spreading on FN (Fig. 6 B upper and lower respectively) with control RAD and RGD peptide occurred, which was comparable to the inhibition of attachment following heparitinase (Fig. 6 A, upper). Moreover, the PKCα inhibitor drastically reduced RGD-independent attachment (over 90%) and spreading (~85%) mediated by the tTG-FN complex (Fig. 6 B), indicating that cell adhesion mediated by tTG-FN critically depends on PKCα activity. This finding also hints at syndecan-4 as the likely HSPG responsible for binding the tTG-FN complex.

RGD-independent adhesion in response to tTG-FN enhances tyrosine phosphorylation of FAK

Having shown that tTG-FN transmits signals via a heparan sulfate receptor leading to cell spreading and that this process depends on the activity of PKCα, we next examined whether the attachment to tTG-FN led to activation of FAK. Tyrosine phosphorylation of FAK in cells plated on FN and treated with RGD peptide was decreased to ~25% that found in control cells plated on FN and pre-incubated with control RAD peptide (Fig. 7). In response to tTG-FN instead, the level of FAK phosphorylation in the presence of RGD peptide was found to be ~60% the level of both control cells on FN or tTG-FN. This data shows that the RGD-independent cell adhesion mediated by tTG-FN enhances tyrosine phosphorylation of FAK and as such implies FAK as one of the intracellular signalling mediators of tTG-FN.

RGD-independent cell adhesion can be mediated by a physiological matrix of cell-assembled FN and cell-secreted tTG

We have previously shown that increased expression of tTG within cells results in an increased export of the enzyme into the extracellular matrix (22, 20, 37, 19). Such a phenomenon has been observed during cell stress and following cell wounding (16, 17). In order to produce such a cell model, conditioned matrices of cell-assembled FN with different bound levels of cell-secreted tTG were obtained from a long-term culture of a transfected fibroblast cell line (Swiss 3T3-TG3), capable of tetracycline (tet) regulatable expression of tTG (22). Cells were then removed from both conditioned matrices, and in their place wild-type Swiss 3T3 fibroblasts were seeded and allowed to adhere in the presence of increasing concentrations of RGD peptide. The FN-rich ECM with increased amounts of cell-secreted tTG (ECM/TG3-tet) (Fig. 8 B). supported significantly higher RGD-independent cell attachment at each RGD peptide concentration, compared to the ECM with background levels of tTG (ECM/TG3+tet) (Fig. 8 A). RGD-independent cell attachment on the lower tTG containing ECM/TG3+tet could be significantly increased by immobilisation of purified tTG on this matrix (ECM/TG3+tet plus tTG) (Fig. 8 A). However, at low levels of RGD peptide, cell attachment was still more effective on the

ECM containing cell-secreted tTG (ECM/TG3-tet) than on the ECM containing added tTG (ECM/tTG3+tet plus tTG). This was despite higher levels of tTG present following exogenous addition of TG (data not shown), suggesting that cell-secreted tTG is better presented to the cell surface. The ECM deposited by cells with increased levels of tTG (ECM/TG3-tet) showed no significant difference in tTG enzymatic activity above background (ECM/TG3+tet) in culture medium, unless in the presence of reducing agent (Fig. 8 C). This is consistent with the idea that tTG activity is gradually downregulated once sequestered in the oxidising extracellular environment.

FN-bound tTG rescues primary dermal fibroblasts from anoikis

A potential physiological function of the tTG-mediated RGD-independent cell adhesion is the protection from apoptosis (anoikis) triggered by inhibition of RGD-dependent adhesion. This phenomenon could occur in tissue injury when changes in the ECM composition lead to reduction of RGD-dependent cell adhesion (8, 5) and the increased externalisation and binding of tTG to the FN matrix in response to wounding (16, 17) may result in an alternative adhesion-dependent survival pathway. Non confluent cultures of mouse dermal fibroblasts devoid of tTG (MDF-TG-/-) were plated on FN or tTG-FN, and incubated with RGD peptide under serum-free conditions. After ~15 h, the majority of the RGD-treated cells plated on FN were detached and displayed morphological signs of apoptosis. The extent of endonucleolysis was measured by fluorescent labelling of DNA strand breaks using TUNEL and quantified by flow cytometry (Fig. 9 A). After incubation with the RGD peptide ~24% of the total fibroblasts grown on FN were apoptotic (black histogram) compared to only ~2.6% of fibroblasts grown on tTG-FN (blue histogram), which behaved similarly to control cells grown on FN in the absence of RGD peptide (green histogram). These data were corroborated by *in situ* fluorescent labelling of nuclei undertaken on the detached cells in suspension, which was visualised and scored by confocal microscopy (Fig. 9 B). At 15 h exposure to the RGD peptide, a significantly lower number of apoptotic cells were found in the culture fluid of cells grown on tTG-FN compared to FN. The level of apoptosis upon incubation on tTG-FN was comparable to that found in the culture medium of control cells on FN without the RGD peptide (Fig. 9 B). After 30 h incubation in the

absence of serum, nuclear fragmentation appeared to increase not only in cells grown with RGD peptide but also in cells grown on FN without RGD peptide, thus limiting our investigations to ~15 h time-period (Fig. 9 B). We next assayed the viability of MDF-TG-/- in response to tTG-FN (Fig. 9 C). Cell viability on FN was significantly decreased after 15-h exposure to RGD peptide, compared to control RAD peptide (Fig. 9 C), in agreement with the level of total apoptotic cell death measured in the same conditions by flow cytometry (Fig. 9 A). In contrast, cell viability on tTG-FN was not substantially altered by incubation with RGD peptide and it was found to be ~30% higher than on FN (Fig. 9 C), indicating that attachment to tTG-FN mediates RGD-independent cell survival.

DISCUSSION

The impact of tTG, a well characterised FN-associating protein and modulator of the FN matrix on FN-mediated cell survival has never been investigated (38). Whereas previous studies have analysed the roles of tTG by modulating its expression (25, 26, 39, 22), in the present study we have developed a model that allows us to characterise cellular responses to a tTG-rich FN matrix, thus mimicking physio/pathological conditions *in vivo*. Support for our model comes from findings that tTG is not only externalised under normal physiological conditions but it is also upregulated, exported and deposited into the ECM in response to tissue trauma following cellular damage, inflammation or cell stress (40, 16, 17), where it either binds FN fibrils directly or plasma FN (20, 22, 24), which is then deposited in the damaged area. Hence a complex of tTG and FN, formed as a result of matrix alterations during tissue injury, may provide a mechanism to ensure adhesion-mediated cell survival in wound-repair in response to the reduction or loss of RGD-dependent cell adhesion (8, 5).

To test this hypothesis, we initially examined the function of the tTG-FN complex in cell-matrix interactions whereby we inhibited the "classical" adhesion-mediated survival pathway dependent on the interaction of the $FNIII_{10}$ RGD cell-binding site with $\alpha_5\beta_1$ integrins. A human osteoblast-like cell line served as the initial cell model since osteoblasts secrete both FN and tTG (34, 30, 41), are subject to continuous matrix remodelling processes during their differentiation, are characterised by a well defined and simple pattern of integrin cell surface receptors, mainly β_1, and make use of RGD-independent pathways in the attachment to the ECM (34). We demonstrate that the loss of cell-matrix interaction by inhibition of RGD-dependent integrin function, can be largely re-established upon seeding of cells on either FN with associated tTG or a more physiological matrix of cell-assembled FN containing cell-secreted tTG. This latter form of tTG-FN matrix is thought to be the most important form present *in vivo* as in tissues, FN is present as an insoluble fibrillar matrix to which tTG is closely associated (22, 20). Restoration of cell adhesion by tTG-FN following RGD inhibition was also found in mouse Swiss 3T3 fibroblasts and in the epithelial-like cells ECV-304, suggesting that

many cell types can use the RGD-independent cell-adhesion pathway mediated by tTG-FN.

We demonstrate that cell adhesion to tTG-FN is not linked to modification of FN by calcium-dependent transamidation. This finding is consistent with recent observations indicating a transamidating-independent role for tTG in cell-matrix interactions (27, 28, 19). Moreover we show that when tTG is complexed with FN it becomes catalytically inactive unless kept in a reduced state. Indeed, previous work has described that tTG sequestration by FN leads to downregulation of enzymatic activity on large-size protein substrates (24). In contrast, *in situ* tTG activity demonstrated with small-size fluorescent primary amine substrate has clearly shown that tTG is catalytically active while present at the cell surface (22). tTG may modify FN by its intrinsic protein disulfide isomerase (PDI) activity, which has been recently ascribed to it (42). However, since GTP-binding to tTG affects the adhesion function of FN-bound tTG but does not affect the PDI activity of tTG this possibility seems unlikely.

The outside-in signalling induced by the RGD-independent cell adhesion to tTG-FN appears to result by direct interaction of tTG with the cell surface, since the blocking of tTG accessibility by a monoclonal antibody greatly reduces this process. The calcium-mediated tertiary structure of tTG is also required, suggesting that crucial cell binding sites might be exposed when tTG assumes the calcium-induced open conformation. However, the simple binding of 20 μg/ml tTG to either tissue culture plastic or the gelatin binding domain of FN, which contains the tTG binding site (13), does not enhance cell adhesion, which is indeed equally negligible regardless of the presence of tTG, in contrast to what has been previously reported (28, 27). We also found that tTG binding to the 70 kd amino-terminal fragment of FN, which can support cell adhesion and includes the tTG binding site, is not sufficient to sustain tTG-mediated RGD-independent cell adhesion. This leads us to conclude that the RGD-independent adhesion to tTG-FN is both tTG and FN dependent, with the amino-terminal of FN required to support tTG binding and the carboxy-terminal of FN and/or cryptic epitopes outside the $FNIII_{9-10}$ domains, essential to sustain the RGD-independent pathway.

Our data also suggest that the RGD-independent cell adhesion to tTG-FN is integrin-independent or, alternatively, the integrin must be in partnership with some other

receptor(s). This observation is supported by the finding that tTG-mediated focal adhesions still formed in the presence of function blocking anti-integrin antibodies β_1 and α_5, which cause conformational inactivation of the receptor, thus preventing outside in signalling (43). Under these conditions the actin stress fibers formed appeared less complex than normal, nevertheless the cytoarchitecture was sufficient for the formation of distinct RGD-independent focal adhesions, which are mediated by GTPase RhoA and induce FAK tyrosine phosphorylation. Therefore, modulation of matrix FN by tTG adds to the increasing number of non-integrin mediated stimuli which enhance FAK activity through actin polymerisation (44). The possibility that tTG-FN may mediate RGD-independent cell adhesion through the $\alpha_4\beta_1$-induced RGD-independent pathway is also unlikely since low or negligible levels of α_4 subunit are generally expressed in osteoblasts (34). Moreover, matrix binding to $\alpha_4\beta_1$ does not generate actin stress fibers (45). Although tTG association with integrins is documented, our data suggest that it is more likely that the cell function induced by tTG-FN results from the binding to non integrin receptors. Given the high affinity binding of tTG for heparin (46), a possible candidate receptor for tTG-FN is that belonging to the class of HSPG (35). Treatment of HOB cells with heparitinase but not chondroitinase ABC, greatly diminished the RGD-independent adhesion in response to tTG-FN, suggesting that cell surface HSPG may mediate RGD-independent cell adhesion to tTG-FN. The C-terminal HepII domain of FN is responsible for the synergistic interaction of FN with cell surface heparan sulfate and integrins and this interaction is essential for optimal cell adhesion and critical for sustained cell survival (7, 35). Association of tTG with FN could induce RGD-independent cell adhesion by reinforcing HSPG-mediated adhesion, through a dual mechanism involving the binding of tTG to cell surface HSPG and increased exposure of the C-terminal heparin-binding domain of FN, which critically depends on FN structure (9). The increased cell spreading observed in osteoblasts and Swiss 3T3 fibroblasts in early cell adhesion to tTG-FN also in the absence of integrin inhibition, suggests that HSPG receptors are not fully occupied when cells are normally seeded on a FN matrix and that increased binding occurs in response to tTG-FN. Downstream signalling from syndecan-4, the only HSPG that is a widespread component of focal adhesion, specifically results in hyperactivation of PKCα and activation of both RhoA and FAK

(7, 35). Our results suggest that RGD-independent cell adhesion mediated by tTG-FN requires PKCα activity since the compound Gö6976, which is the only inhibitor available that shows specificity for PKCα (36), blocks this process. Our data also show that the function of FN-bound tTG depends on RhoA activation and is linked to activation of the cell survival kinase FAK (1, 44).

Moreover, in preliminary investigations using a Raf-1 null 3T3 like immortalised fibroblast cell line (47) we could demonstrate that the RGD-independent cell adhesion pathway by tTG-FN is not functional in this cell line (unpublished data). This suggests that the Raf-1 protein, whose main function is anti apoptotic (47), may be a key component in the signalling pathway mediated by tTG-FN. The observation that a tTG-FN matrix can rescue tTG-null primary dermal fibroblasts from anoikis with maintenance of cell viability is therefore consistent with its activation of intracellular survival mediators. Importantly, it shows that the survival role of tTG is essentially extracellular and not intracellular as recently suggested by Antonyak et al (2001) (48), following upregulation of tTG by retinoic acid.

It is now accepted that RGD-mediated cell adhesion is not sufficient in isolation to maintain cell survival. For sustained survival cells need to interact with "complex" ECMs via integrin and non-integrin receptors, such as cell surface proteoglycans (7). Interestingly like tTG, increased expression of syndecan-4 is also found at sites of tissue injury (35). The work presented here indicates that binding of tTG to FN represents one additional survival signal by inducing heparan-sulfate receptors-mediated cell adhesion, which can either act in synergy or in alterative to integrin RGD-dependent cell adhesion at sites of tissue injury.

ACKNOWLEDGEMENTS

The authors thank Dr M Baccarini (Vienna Biocenter, Austria) for critically reading the manuscript and for donating the Raf-1 null 3T3-like immortilised fibroblasts, and M Stevenson for help with the compilation of the manuscript. This work was partially supported by grants from EPSRC (GR/L43688), Telethon (E872, E1224), AIRC, EU and MIUR.

REFERENCES

1. Frisch, S. M., and Screaton, R. A. (2001) *Curr. Opin. Cell Biol.* **13,** 555-562
2. Boudreau, N., Sympson, C. J., Werb, Z., and Bissell, M.J. (1995) *Science.* **267,** 891-893
3. Davis, G. E., Bayless, K. J., Davis, M. J., and Meininger, G. A. (2000) *Am. J. Pathol.* **156,** 1489-1498
4. Sechler, J. L., and Schwarzbauer, J. E. (1998) *J. Biol. Chem.* **273,** 25533-25536
5. Hadden, H.L., and Henke, C.A. (2000) *Am. J. Respir. Crit. Care Med.* **162,** 1553-1560
6. Buckley, C. D., Pilling, D., Henriquez, N. V., Parsonage, G., Threlfall, K., Scheel_Toellner, D., Simmons, D. L., Akbar, A. N., Lord, J. M., and Salmon, M. (1999) *Nature* **397,** 534-539
7. Jeong, J., Han, I., Lim, Y., Kim, J., Parks, I., Wood, A., Couchman, J. R., and Oh, E. S. (2001) *Biochem. J.* **356,** 231-537
8. Kapila, Y. L., Wang, S., and Johnson, P.W. (1999) *J. Biol. Chem.* **274**, 30906-30913
9. Sharma, A., Askari, J. A., Humphries, M. J., Jones, E. Y., and Stuart, D. I. (1999) *EMBO J.* **18,** 1468-1479
10. Aeschlimann, D., and Thomazy, V. (2000) *Connect. Tissue Res.* **41,** 1-27
11. Pereira, M, Rybarczyk, B. J., Odrljin, T. M., Hocking, D. C., Sottile, J., and Simpson-Haidaris, P. J. (2002) *J. Cell Sci.* **115,** 609-617
12. Hocking, D. C., Sottile, J., and Langenbach, K. J. (2000) *J. Biol. Chem.* **275,** 10673-10682
13. Radek, J. T., Jeong, J. M., Murthy, S. N., Ingham, K. C., and Lorand, L. (1993) *Proc. Natl. Acad. Sci. USA.* **90,** 3152-3156
14. Griffin, M., Casadio, R., and Bergamini, C. M. (2002) *Biochem. J. Rev.* **368,** 377-396
15. Fesus, L., and Piacentini, M. (2002) *Trends Biochem. Sci*. **27,** 534-539
16. Haroon, Z. A., Hettasch, J. M., Lai, T. S., Dewhirst, M. W., and Greenberg, C. S. (1999) *FASEB J.* **13,** 1787-1795

17. Johnson, T. S., Skill, N. J., El Nahas, A. M., Oldroyd, S. D., Thomas, G. L., Douthwaite, J. A., Haylor, J. L., and Griffin, M. **(**1999) *J. Am. Soc. Nephrol.* **10,** 2146-2157
18. Liu, S., Cerione, R. A., and Clardy, J. (2002) *Proc. Natl. Acad. Sci. USA.* **99,** 2743-2747
19. Balklava, Z., Verderio, E., Collighan, R., Gross, S., Adams, J., and Griffin, M. (2002) *J. Biol. Chem.* **277,** 16567-16575
20. Gaudry, C. A., Verderio, E., Aeschlimann, D., Cox, A., Smith, C., and Griffin, M. (1999) *J. Biol. Chem.* **274,** 30707-30714
21. Jeong, J. M., Murthy, S. N., Radek, J. T., and Lorand L. (1995) *J. Biol. Chem.* **10**, 5654-5658
22. Verderio, E., Nicholas, B., Gross, S., and Griffin, M. (1998) *Exp. Cell Res.* **239,** 119-138
23. Belkin, A. M., Akimov, S. S., Zaritskaya, L. S., Ratnikov, B. I., Deryugina, E. I., and Strongin, A. Y. (2001) *J. Biol. Chem.* **276,** 18415-18422
24. LeMosy, E. K., Erickson, H. P., Beyer, W. F., Radek, J. T., Jeong, J. M., Murthy, S. N., and Lorand, L. (1992) *J. Biol. Chem.* **267,** 7880-7885
25. Gentile, V., Thomazy, V., Piacentini, M., Fesus, L., and Davies, P. J. (1992) *J. Cell Biol.* **119,** 463-474
26. Jones, R. A., Nicholas, B., Mian, S., Davies, P. J., and Griffin, M. (1997) *J. Cell Sci.* **110,** 2461-2472
27. Akimov, S. S., Krylov, D., Fleischman, L. F., and Belkin, A. M. **(**2000) *J. Cell Biol.* **148,** 825-838
28. Takahashi, H., Isobe, T., Horibe, S., Takagi, J., Yokosaki, Y., Sheppard, D., and Saito, Y. (2000) *J. Biol. Chem.* **275,** 23589-23595
29. Leblanc, A., Day, N., Menard, A., and Keillor, J. W. *Protein Expr. Purif.* **17,** 89-95
30. Verderio, E., Coombes, A., Jones, R. A., Li, X., Heath, D., Downes, S., and Griffin, M. (2000) *J. Biomed. Mat. Res.* **54**, 294-304
31. De Laurenzi, V., and Melino, G. (2001) *Mol. Cell Biol.* **21,** 148-155

32. Dedhar, S., Ruoslahti, E., and Pierschbacher, M. D. (1987) *J. Cell Biol.* **104,** 585-593
33. Heath, D. J., Christian, P., and Griffin, M. (2002) *Biomaterials.* **23,** 1519-1526
34. Gronthos, S., Stewart, K., Graves, S. E., Hay, S., and Simmons, P. J. (1997) *J. Bone Miner. Res.* **12,** 1189-1197
35. Woods, A., and Couchman, J. R. (2001) *Curr. Opin. Cell Biol.* **13,** 578-583
36. Gschwendt, M., Dieterich, S., Rennecke, J., Kittstein, W., Muller, H. J., and Johannes, F. J. (1996) *FEBS Lett.* **392,** 77-80
37. Verderio, E., Gaudry, C. A., Gross, S., Smith, C., Downes, S., and Griffin, M. (1999) *J. Histochem Cytochem.* **47,** 1417-1432
38. Lorand, L., and Graham, R. M. (2003) *Nat Rev Mol Cell Biol*. **4**, 140-156
39. Melino, G., Thiele, C. J., Knight, R. A., and Piacentini, M. (1997) *J. Neurooncol.* **31,** 65-83
40. Upchurch,H. F., Conway, E., Patterson, M. K., Jr., and Maxwell, M. D. (1991) *J. Cell Physiol*. **149,** 375-382
41. Heath, D. J., Downes, S., Verderio, E., and Griffin, M. (2001) *J. Bone Miner. Res.* **8,** 1477-1485
42. Hasegawa, G., and Saito, Y. (2002) *Minerva Biotecnologica.* **14,** 192
43. Humphries, M. J. (2000) *Trends Pharmacol. Sci.* **21,** 29-32
44. Schlaepfer, D. D., Hauck, C. R., and Sieg, D. J. (1999) *Prog. Biophys. Mol. Biol.* **71,** 435-478
45. Sechler, J. L., Cumiskey, A. M., Gazzola, D. M., and Schwarzbauer, J. E. (2000) *J. Cell Sci.* **113,** 1491-1498
46. Bergamini, C. M., and Signorini, M. (1993) *Biochem. J.* **291,** 37-39
47. Mikula, M., Schreiber, M., Husak, Z., Kucerova, L., Ruth, J., Wieser, R., Zatloukal, K., Beug, H., Wagner, E. F., and Baccarini, M. (2001) *EMBO J.* **20,** 1952-1962
48. Antonyak, M. A., Singh, U. S., Lee, D. A., Boehm, J. E., Combs, C., Zgola, M. M., Page, R. L., and Cerione, R. A. (2001) *J. Biol. Chem.* **276,** 33582-33587

ABBREVIATIONS

The abbreviations used are: ECM, extracellular matrix; FN, fibronectin; HSPG, heparan sulfate proteoglycans; tTG, tissue transglutaminase; PKCα, protein kinase Cα; HOB, human osteoblasts; DMEM, Dulbecco's modified Eagle's medium; FCS, fetal calf serum; MDF, mouse dermal fibroblasts; TCP, tissue culture plastic; ELISA, enzyme-linked immunosorbent assay; PBS, phosphate-buffered saline; PFM, paraformaldehyde; FITC, fluorescein isothiocyanate; BSA, bovine serum albumine; tet, tetracycline; TUNEL, TdT-mediated dUTP nick end labeling; TdT, terminal deoxynucleotidyl transferase.

FIGURE LEGENDS

Figure 1

tTG bound to FN but not tissue culture plastic supports RGD-independent cell adhesion.

(A) Relative levels of tTG bound to coated FN at increasing concentrations of free tTG. Data are expressed as mean ± SD absorbance at 450nm and represent one typical experiment undertaken in triplicate. Background absorbance (in the range of 0.02-0.15) was subtracted from data. The level of tTG bound to fibronectin (FN) after incubation with 20 μg/ml free tTG is significantly different from the level after incubation with 10 μg/ml, but not 30-50 μg/ml tTG. The level of tTG bound to tissue culture plastic (TCP) represents the positive experimental control. (B) RGD-independent cell adhesion of HOB cells and (C) Swiss 3T3 fibroblasts in response to tTG-FN. Cell attachment (upper graphs in B and C) and cell spreading (lower graphs in B and C) on FN and tTG-FN were assessed 20 min after seeding cells pre-incubated with increasing concentrations of RGD synthetic peptide (0-200 μg/ml) (RGD 0-200), as described in the "Experimental Procedures". Insets in B and C show cell attachment (upper insets) and spreading (lower insets) on FN when cells were pre-incubated with equivalent concentrations of control RAD peptide (RAD 0-200). Each point represents the mean number of attached cells (cell attachment) or the mean percentage of spread cells (cell spreading) ±SD. Data are expressed as percentage of control values on FN, which represents 100% and represent one of at least 3 separate experiments performed in triplicate. Mean attachment values ±SD on FN control were 306±53 (HOB) and 166±3 (Swiss 3T3) in upper graphs, 246±13 (HOB) and 155±14 (Swiss 3T3) in upper insets; mean percentage values of spread cells on FN control were 78±5 (HOB) and 88±1 (Swiss 3T3) in lower graphs and 82±2 (HOB) and 86±3 (Swiss 3T3) in lower insets; total cells analysed in control sample were ~900 (HOB) and ~500 (Swiss 3T3). (D) Comparison of HOB cell attachment to TCP with increasing concentrations of bound tTG (20-50 μg/ml) and TCP with bound FN (5 μg/ml) in complex with tTG (20-50 μg/ml). Cell attachment was assessed and expressed as described above (RGD peptide was 100 μg/ml). Mean attachment values ±SD on FN

control were 214±22. Total cells analysed in control sample were ~700. RGD-independent cell attachment to TCP with bound tTG did not significantly differ from cell attachment to TCP at any tTG concentration.

Figure 2

tTG immobilisation on amino-terminal FN fragments is not sufficient to mediate RGD-independent cell adhesion.

(A) Relative levels of tTG bound to the amino-terminal FN fragments (70 kd, 45 kd, and 30 kd) immobilised on TCP, at increasing concentrations of free tTG. Data are expressed as mean ± SD absorbance at 450nm and are from a typical experiment performed in triplicate. The level of tTG bound to each fragment after incubation with 20 μg/ml tTG was not significantly different from the level bound using 30 μg/ml. (B) Assessment of cell adhesion in response to tTG bound to amino-terminal FN fragments. Wells were pre-coated with amino-terminal FN fragments and in half of the wells 20 μg/ml tTG was immobilised upon them (TG-70, TG-45, TG-30). Cell attachment (B upper) and cell spreading (B lower) of HOB cells pre-incubated with RGD peptide (100 μg/ml) (+RGD) or DMEM (-RGD) were assessed and data expressed as described in legend to Fig. 1. In B upper, ordinate represents mean cell attachment expressed as mean percentage of control attachment to FN (which represents 100%) ±SD of 3 independent experiments undertaken in triplicate (mean attachment value ±SD on FN in the 3 experiments was 406±72, 370±49, 465±51; total cells analysed in control samples were respectively ~1200, ~1100, ~1400). In B lower, ordinate represents the mean percentage of spread cells, expressed as mean percentage of control spreading on FN ±SD of 3 independent experiments undertaken in triplicate (mean percentage of spreading ±SD on FN in the 3 experiment was 87±1, 91±1, 88±7).

Figure 3

Confocal laser fluorescence microscopy of RGD-independent actin cytoskeleton organisation and focal adhesion in response to tTG-FN.

(A) Visualisation of actin stress fibers and focal adhesions in the presence of RGD peptide. Cells were seeded as in legend to Fig. 1 and the indicated cells pre-treated with

RGD peptide (100 μg/ml) (RGD). Actin stress fibres and focal adhesions were revealed as described in the "Experimental Procedures". Images were acquired by confocal laser fluorescence microscopy and cells in random fields (at least 100 cells in FN control) were scored for actin stress fiber formation as outlined in the "Experimental Procedures". Data shown in the histogram are from a representative experiment. Ordinate represents the mean percentage of cells with formed actin stress fibers expressed as percentage of control values on FN. Mean ±SD percentage of cells with stress fibers formed on control FN was 74±2. *Arrows* point at tTG-FN mediated stress fibers with and without RGD peptide. Bars 10 μM. (B) Actin stress fibers in the presence of function blocking anti-integrin α_5 and β_1 antibodies. HOB cells in suspension were pre-incubated with anti-integrin antibodies P1D6 (α_5) and JB1A (β_1) or control mouse IgGs (IgG) before seeding on either FN or tTG-FN as described in A. At least 200 cells in FN/IgG control were scored. Mean percentage value of cells with actin fibers formed on control FN ±SD was 49±8.4 in B upper and 53±7.8 in B lower graph. Bars 10 μM (C) Relative measurement of actin stress fibers following pre-incubation with the RhoA inhibitor C3 exotransferase. Monolayers of HOB cells were loaded with C3 exotransferase (C3), or lipofectin only (Lpf), as described in the "Experimental Procedures" and then seeded as described in A. At least 250 cells in FN/Lpf control were scored. Mean percentage value of cells with actin fibers formed on control FN ±SD was 63±5.

Figure 4

tTG cross-linking activity is not required to support RGD-independent cell adhesion to tTG-FN.

(A) The activity of FN-bound tTG (TG-FN) was measured by incorporation of biotinylated cadaverine into FN in either culture medium DMEM (DM), or DMEM with 5 mM Ca^{2+} (DM-Ca^{2+}) or DMEM supplemented with 5 mM DTT (DM-DTT). Values represent the mean ± SD absorbance at 450nm of one typical experiment undertaken in triplicate. (B) Cell adhesion to tTG-FN following inactivation of tTG. The tTG-FN matrix was incubated with the tTG irreversible inhibitor R283 (100 μM), and then utilised as adhesive substrate for HOB cells, further supplemented with the same concentration of R283. In controls, identically treated cells were seeded on tTG-FN

without R283 treatment. Where indicated, cells were pre-incubated with RGD peptide (100 μg/ml). Cells were examined for cell attachment (B upper) and cell spreading (B lower) and data expressed as percentage of control values on FN as in Fig. 1. Mean attachment value on FN control ±SD, 373±36 in B upper; mean percentage value of spread cells ±SD on FN control, 89±6 in B lower; total cells analysed in control sample, ~1100. Data shown are from a representative experiment undertaken in triplicate. (C) Inhibition of the cross-linking activity of FN-bound tTG (TG-FN) and tTG free in solution (fTG) by 100 μM R283, when measured as described in A, in buffer containing DTT. Values represent the mean ± SD of a representative experiment undertaken in triplicate.

Figure 5

RGD-independent cell adhesion to FN-bound tTG depends on tTG accessibility and GTP-mediated conformational change.

(A) FN-bound tTG was blocked by incubation with Cub74 (40 μg/ml) for 1 h at 37 °C in PBS with 2 mM EDTA using mouse IgG1k as control antibody. Following pre-incubation with RGD peptide, cells were seeded on the tTG-FN matrix. Adhered cells were examined for cell attachment (A upper) and cell spreading (A lower) and data expressed as in legend to Fig. 1. Mean attachment value ±SD on FN control, 229±13 in A upper; mean percentage value of spread cells ±SD on FN control, 93±2 in A lower; total cells analysed in control sample, ~700. Data are from a typical experiment undertaken in triplicate. (B) Availability of FN, detected as described in the "Experimental Procedures", after blocking the tTG-FN matrix by Cub74 and IgG1k. Values represent the mean ± SD absorbance at 450nm of 4 replicates from a typical experiment. (C) HOB cells in suspension, pre-incubated with RGD peptide (100 μg/ml) as indicated, were seeded in the presence of 1 mM GTP-γS on FN-bound tTG, pre-incubated with 1mM GTP-γS in PBS for 10 min at room temperature. Adhered cells were examined for cell attachment (C upper) and cell spreading (C lower) with and without inactivation of tTG by GTP-γS and data expressed as in legend to Fig. 1. Mean attachment value ±SD on FN control, 294±98.32 in C upper; mean percentage value of spread cells ±SD on FN control, 84.9±4 in C lower; total cells analysed in control sample, ~800. Data are from a typical

experiment undertaken in triplicate. (D) Relative levels of tTG that bind FN in the presence of 1 mM GTP-γS, in conditions identical to C above. tTG was detected by an ELISA-type assay described in the "Experimental Procedures". Values represent the mean ± SD absorbance at 450nm of 4 replicates from a representative experiment.

Figure 6

RGD-independent cell adhesion to tTG-FN is dependent on cell surface heparan sulfate and PKCα activity

(A) HOB cells in suspension ($2x10^5$ cell/ml) were pre-treated with 15 mU/ml heparitinase or 15 mU/ml protease-free chondroitinase ABC in serum-free medium for 1 h at 37 °C before evaluating cell attachment (upper) and cell spreading (lower) in the presence of RGD or RAD peptide (100μg/ml). Data are produced and expressed as in legend to Fig. 1 and represent percentage of control values on FN from one of 3 separate experiments. Mean attachment values ±SD on FN control without peptide treatment (not shown), 140±16; mean percentage values of spread cells on FN control, 89±2; total cells analysed in control sample, ~420. (B) Monolayers of sub-confluent HOB cells were serum-starved for 12 h and then incubated in serum-free DMEM medium supplemented with the PKCα inhibitor Gö6976 (5 μM, dissolved in DMSO) for 1 h or with an equal volume of DMSO only. Cells were then harvested and analysed for cell attachment (upper) and spreading (lower) on FN and tTG-FN. Data, expressed as percentage of control values on FN, are from one of 3 separate experiments. Mean attachment and spread cell values ±SD on FN control without peptide (not shown), 197±8 and 83±4, respectively; total cells analysed in control sample, ~590.

Figure 7

RGD-independent adhesion to tTG-FN promotes tyrosine phosphorylation of FAK.

Lysates of HOB cells grown in the presence of RGD or RAD control peptide (100 μg/ml) on FN, tTG-FN or control BSA-coated TCP, were western blotted and then immunoprobed with phospho(Tyr397)-FAK antibody followed by peroxidase conjugate anti-rabbit IgG (FAK-PY), as described in the "Experimental Procedures". After

stripping, blots were re-probed to reveal control protein tubulin (Tub). Density of bands was quantified by scanning densitometry, and phospho-FAK bands normalised against values for tubulin bands (relative FAK-PY). Results from one of 3 typical experiments are shown.

Figure 8

A physiological matrix of FN and cell-secreted tTG supports RGD-independent cell adhesion of Swiss 3T3 fibroblasts.

(A) Swiss 3T3-TG3 cells were grown on TCP either in the absence of tet, to induce the expression of tTG and deposit a ECM rich in tTG (ECM/TG3-tet), or in the presence of tet, to inhibit tTG overexpression and deposit a ECM with background levels of tTG (ECM/TG3+tet). Cells were then removed by 5 mM EDTA in PBS, and the remaining matrices used to measure the attachment of wild-type Swiss 3T3 fibroblasts, pre-incubated with increasing concentrations of RGD peptide (30-100 μg/ml). RGD-independent adhesion was also tested on ECM/TG3+tet supplemented with purified tTG (20 μg/ml), which was immobilised as done on purified FN (ECM/TG3+tet plus TG). Each point represents the mean number of attached cells ±SD of a representative experiment performed in triplicate. (B) Relative levels of tTG in the ECM of cells overexpressing tTG (TG3-tet) and with background tTG (TG3+tet). tTG was detected by an ELISA-type assay described in the "Experimental Procedures". Values represent the mean ± SD of 6 replicates from a representative experiment. (C) Cross-linking activity of tTG in ECM/TG3+tet and ECM/TG3-tet, measured by the incorporation of biotinylated cadaverine into FN in culture medium DMEM in the absence (DM) or presence of 5 mM DTT (DTT). Data represent the mean ± SD of 3 replicates from a typical experiment.

Figure 9

Cell attachment to tTG-FN promotes cell survival of tTG-null dermal fibroblasts induced to undergo apoptosis by inhibition of RGD-dependent integrin function

(A) Flow cytometric analysis of apoptosis in tTG-null mouse dermal fibroblasts (MDF-TG-/-). Cells were seeded in medium containing RGD peptide (100 μg/ml) or DMEM only, on FN or tTG-FN for 15 h. As a measure of apoptosis, nuclear fragmentation of

both adherent and detached cells was detected by TUNEL and quantified by flow cytometry as described in the "Experimental Procedures". The bar denotes the positive region of fragmented nuclei (% apoptotic nuclei), set by the negative standard (n.s.) of cells undergoing anoikis and incubated with FITC-dUTP in the absence of the enzyme TdT (red histogram). Md, median fluorescence channel. (B) *In situ* analysis of nuclear fragmentation of MDF-TG-/-. Cells were treated with RGD peptide and incubated as described in A. After 15 h and 30 h growth, the fractions of cells in suspension were processed for *in situ* detection of DNA fragmentation, which was scored by confocal fluorescent microscopy as described in the "Experimental Procedures". Data represent the mean number ±SD of apoptotic cells/well from a typical experiment undertaken in triplicate. Total cells analysed, ~450 and ~400 at 15 h and 30 h, respectively. Bar 10 μM. (C) Cell viability assay of MDF-TG-/-. Cells were grown in medium containing RGD or control RAD peptide (100 μg/ml) on FN or tTG-FN for 15 h, as described above. Cell viability was tested following incubation of cells with XTT. Data represent the mean ± SD of a typical experiment performed in quadruplicate.

Figure 1

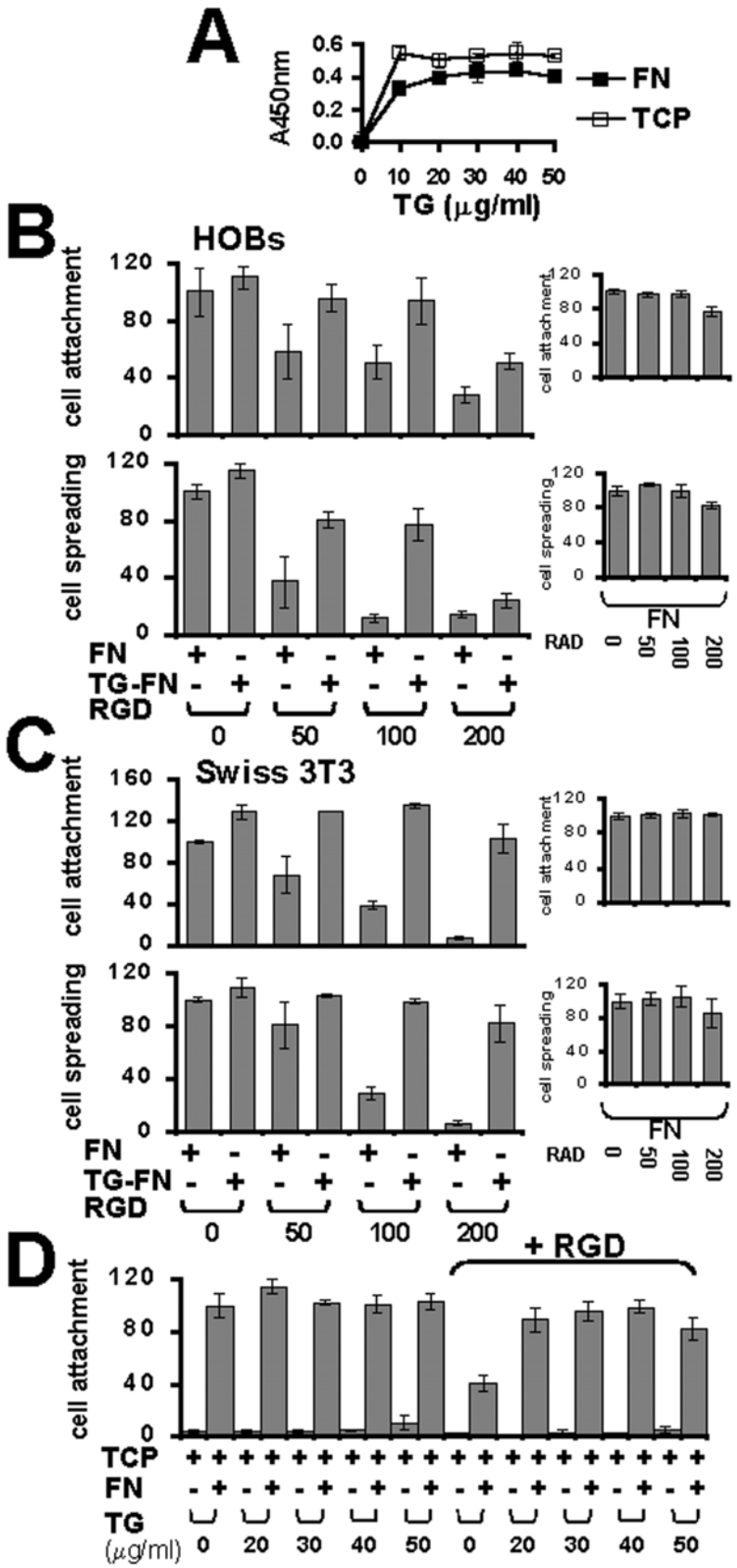
A
A450nm
0.6
0.4
0.2
0.0
0 10 20 30 40 50
TG (μg/ml)
FN
TCP
B
HOBs
cell attachment
cell spreading
120
80
40
0
FN + - + - + - + -
TG-FN - + - + - + - +
RGD
0 50 100 200
RAD 0 50 100 200
C
Swiss 3T3
160
D
+ RGD
TCP + + + + + + + + + + + + + + + + + +
FN - + - + - + - + - + - + - + - + - +
TG
(μg/ml) 0 20 30 40 50 0 20 30 40 50

Figure 2

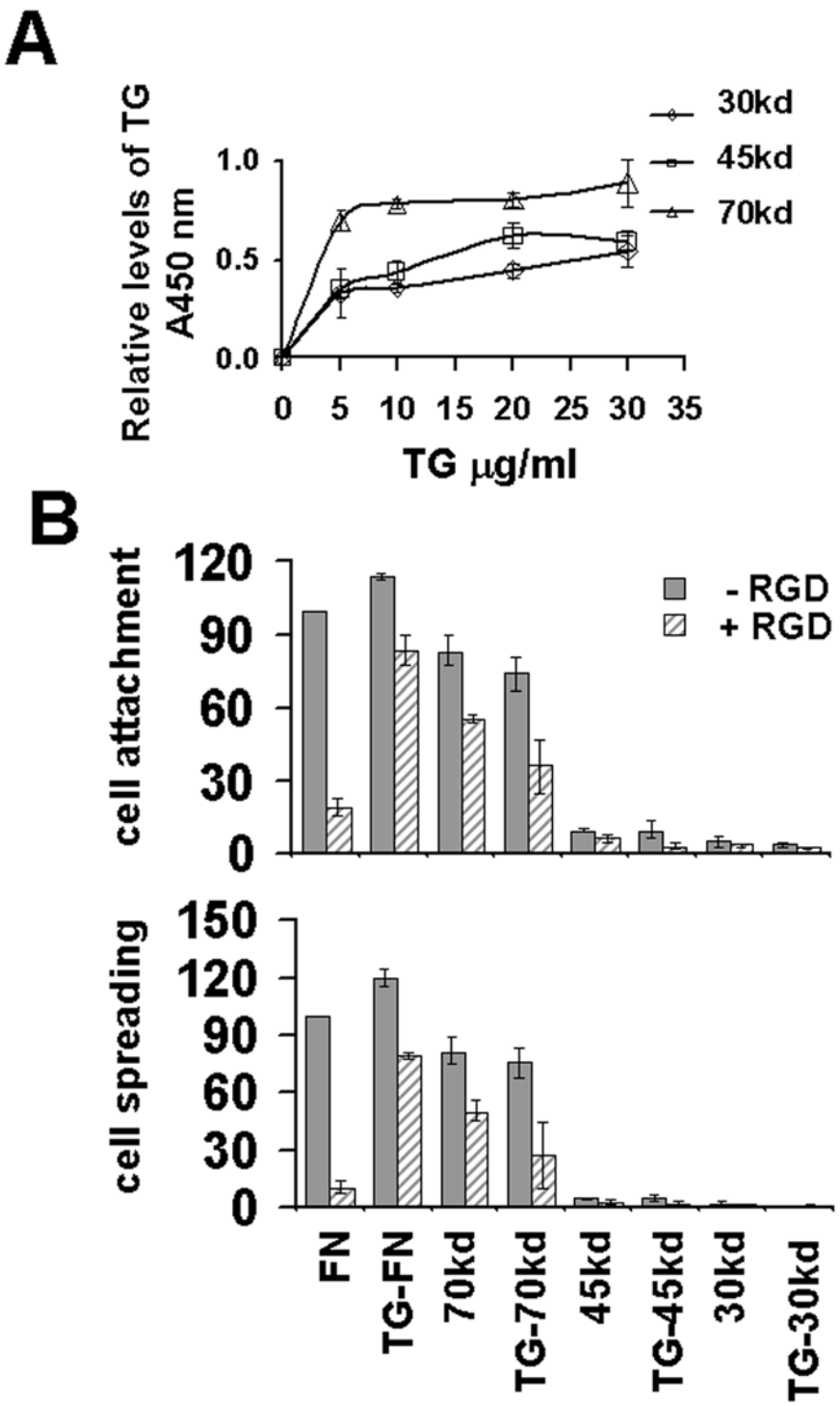
A
Relative levels of TG A450 nm
1.0
0.5
0.0
0 5 10 15 20 25 30 35
TG μg/ml
30kd
45kd
70kd
B
cell attachment
120
90
60
30
0
- RGD
+ RGD
cell spreading
150
120
90
60
30
0
FN
TG-FN
70kd
TG-70kd
45kd
TG-45kd
30kd
TG-30kd

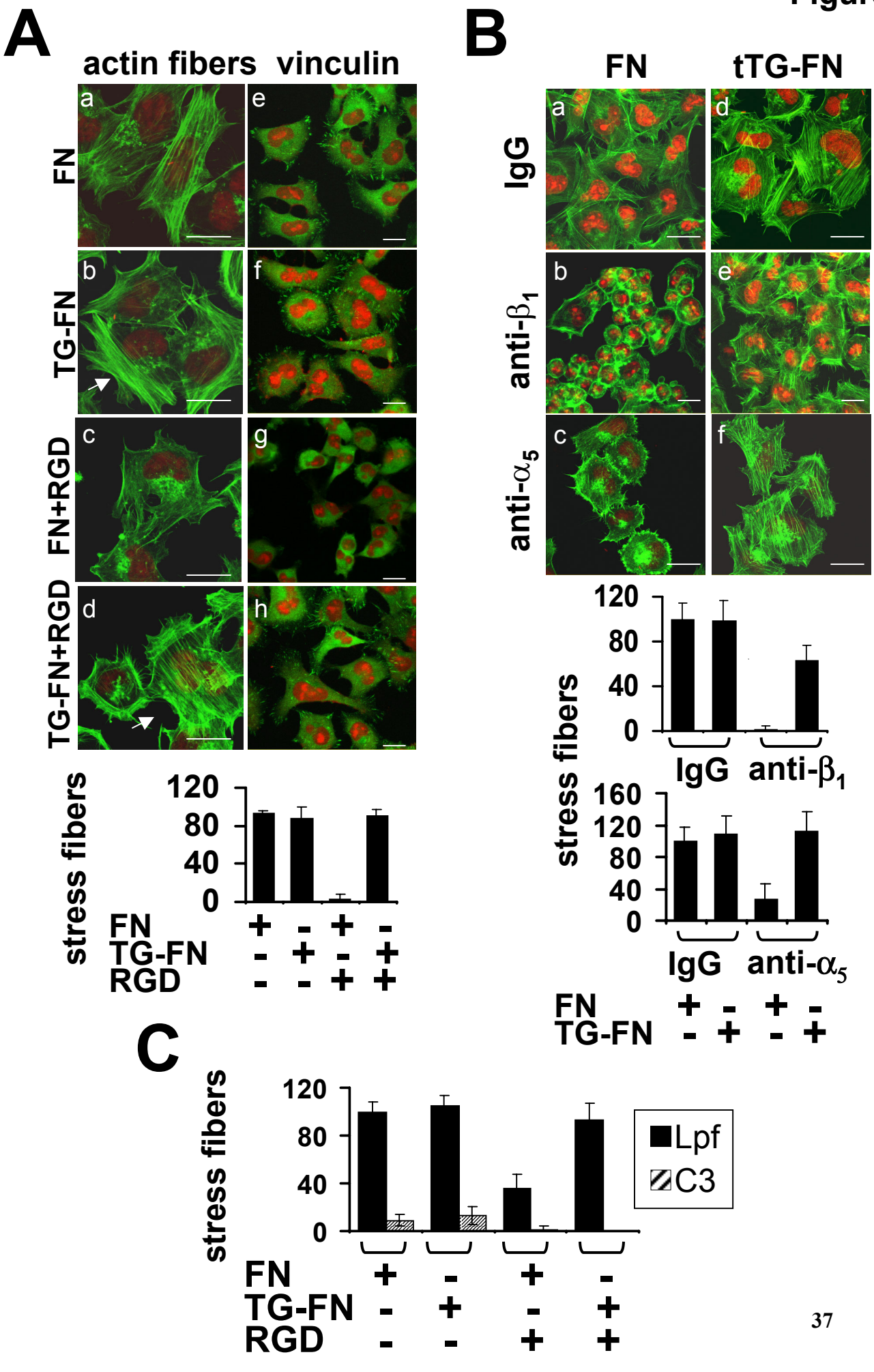
A
actin fibers
vinculin
FN
TG-FN
FN+RGD
TG-FN+RGD
a
b
c
d
e
f
g
h
stress fibers
120
80
40
0
FN
TG-FN
RGD
B
FN
tTG-FN
IgG
anti-β1
anti-α5
a
b
c
d
e
f
stress fibers
120
80
40
0
IgG
anti-β1
160
120
80
40
0
IgG
anti-α5
FN
TG-FN
C
stress fibers
120
80
40
0
Lpf
C3
FN
TG-FN
RGD

Figure 4

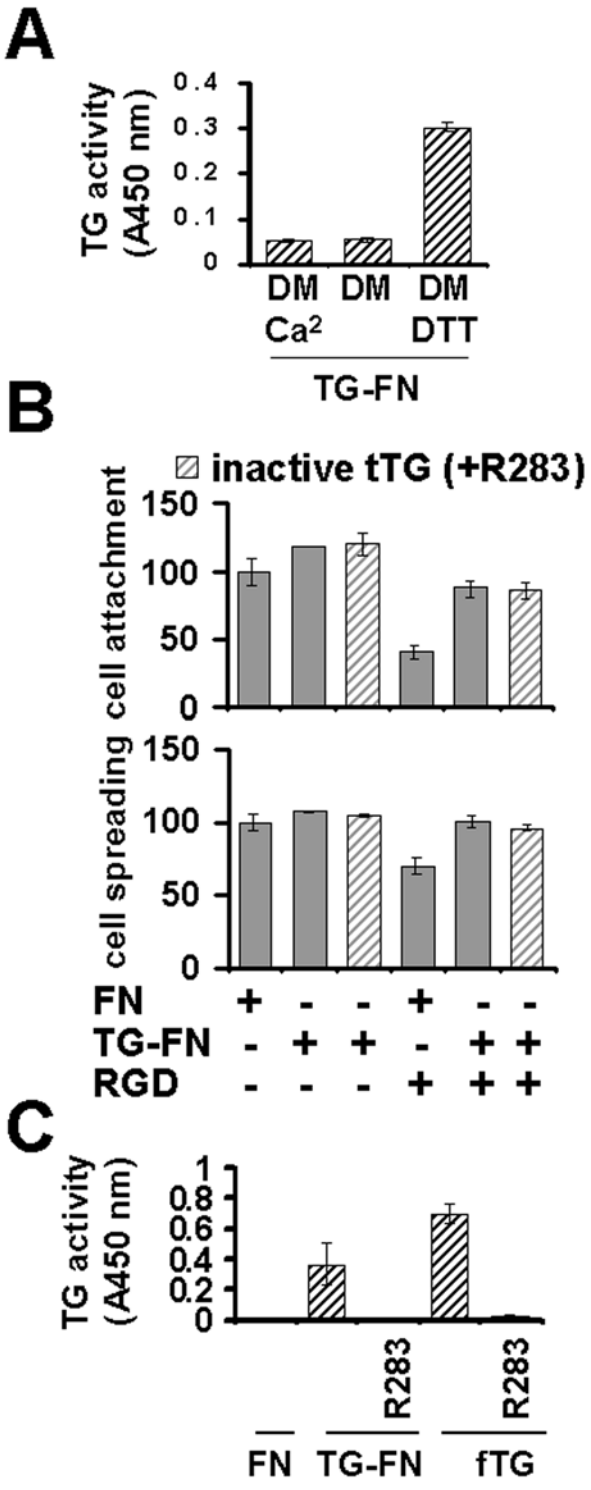
A
TG activity (A450 nm)
0.4
0.3
0.2
0.1
0
DM Ca2
DM
DM DTT
TG-FN
B
inactive tTG (+R283)
cell attachment
150
100
50
0
cell spreading
150
100
50
0
FN + - - + - -
TG-FN - + + - + +
RGD - - - + + +
C
TG activity (A450 nm)
1
0.8
0.6
0.4
0.2
0
R283
R283
FN
TG-FN
fTG

Figure 5

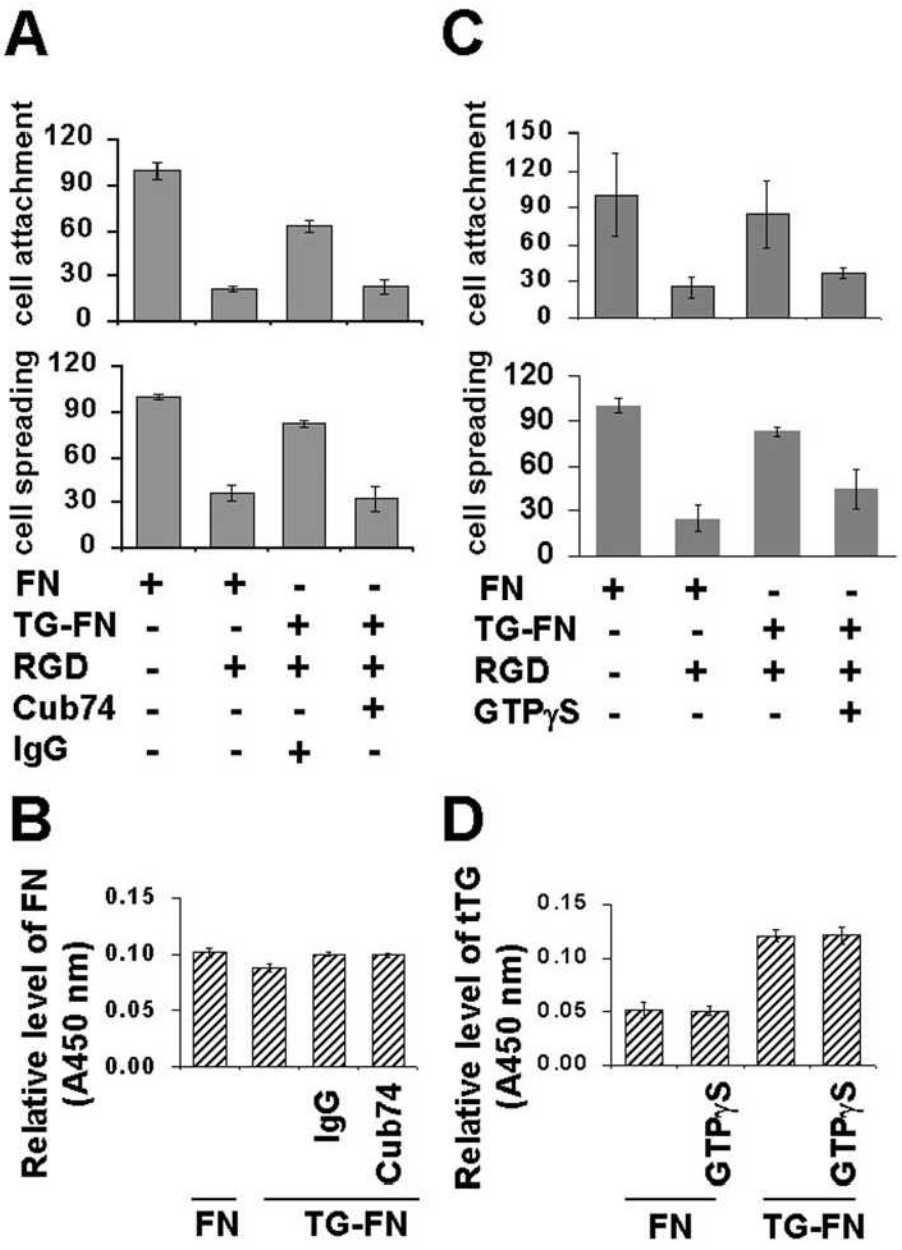
A
cell attachment
120
90
60
30
0
cell spreading
120
90
60
30
0
FN + + - -
TG-FN - - + +
RGD - + + +
Cub74 - - - +
IgG - - + -
C
cell attachment
150
120
90
60
30
0
cell spreading
120
90
60
30
0
FN + + - -
TG-FN - - + +
RGD - + + +
GTPγS - - - +
B
Relative level of FN (A450 nm)
0.15
0.10
0.05
0.00
IgG
Cub74
FN
TG-FN
D
Relative level of tTG (A450 nm)
0.15
0.10
0.05
0.00
GTPγS
GTPγS
FN
TG-FN

Figure 6

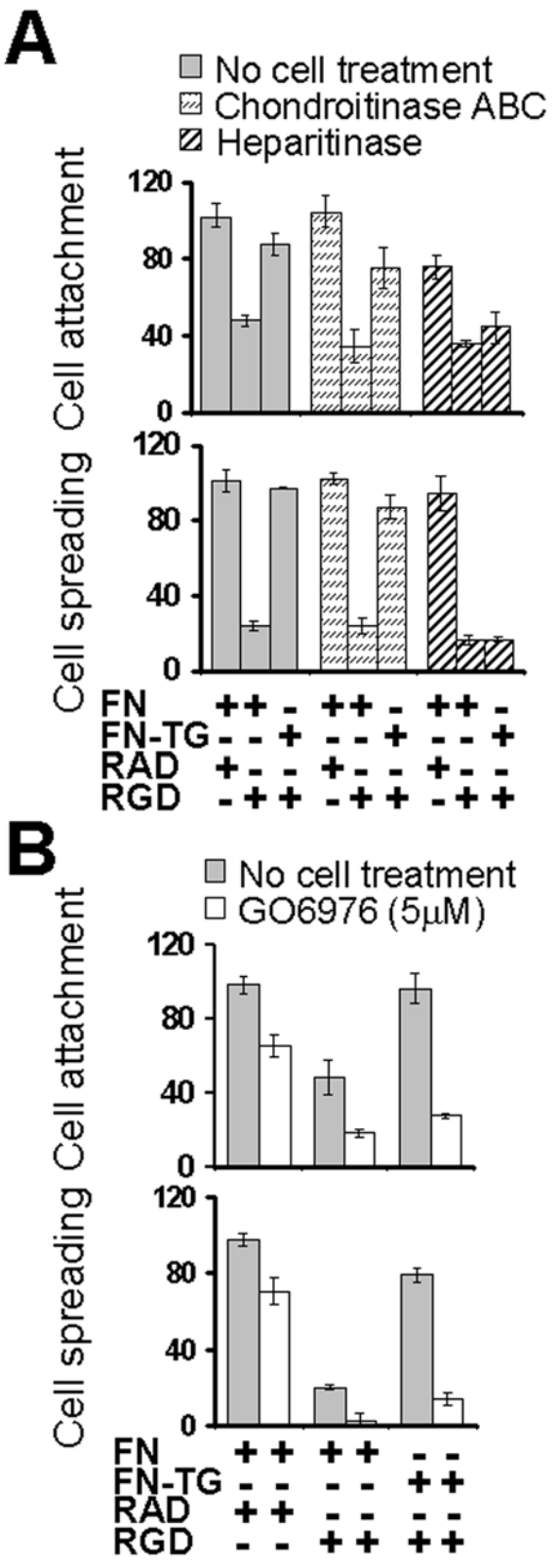

Figure 7

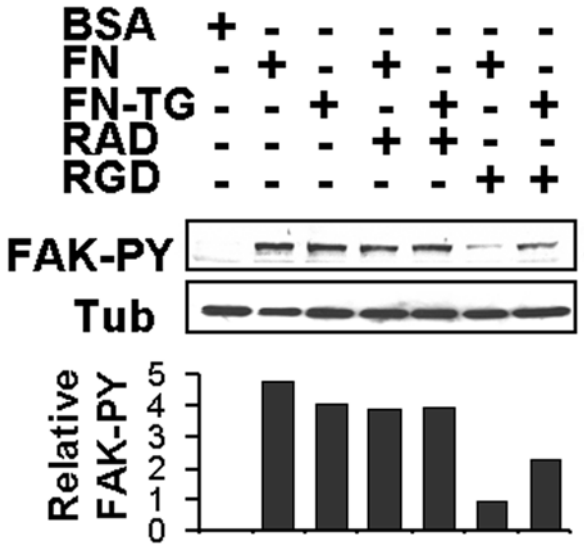

Figure 8

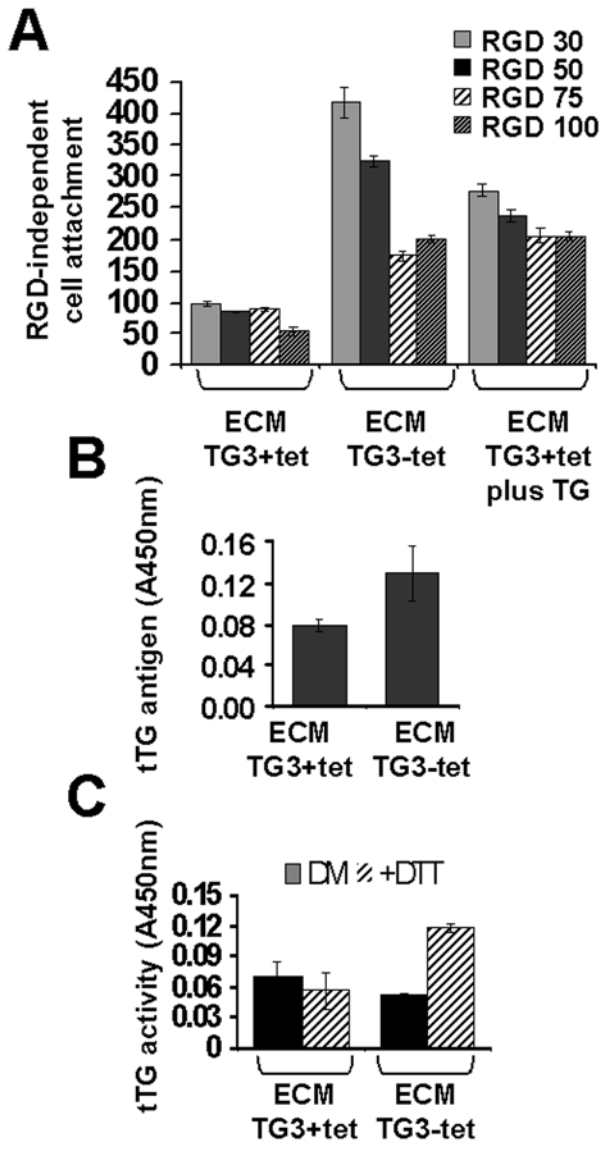

Figure 9

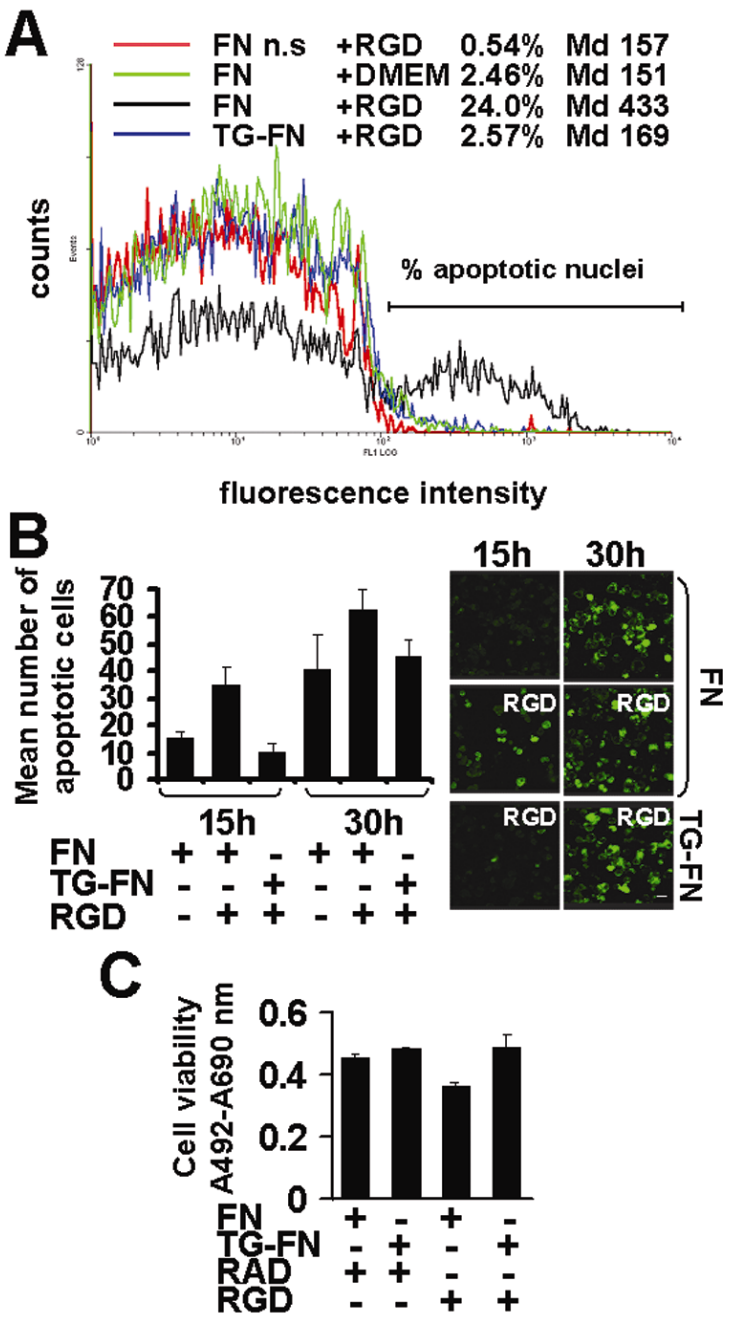
A
FN n.s +RGD 0.54% Md 157
FN +DMEM 2.46% Md 151
FN +RGD 24.0% Md 433
TG-FN +RGD 2.57% Md 169
counts
% apoptotic nuclei
fluorescence intensity
B
Mean number of apoptotic cells
70
60
50
40
30
20
10
0
15h
30h
FN + + - + + -
TG-FN - - + - - +
RGD - + + - + +
15h
30h
RGD
FN
TG-FN
C
Cell viability A492-A690 nm
0.6
0.4
0.2
0
FN + - + -
TG-FN - + - +
RAD + + - -
RGD - - + +

SUPPLEMENTAL DATA

Figure S1
RGD-independent adhesion to tTG-FN of epithelial-like cell line ECV-304

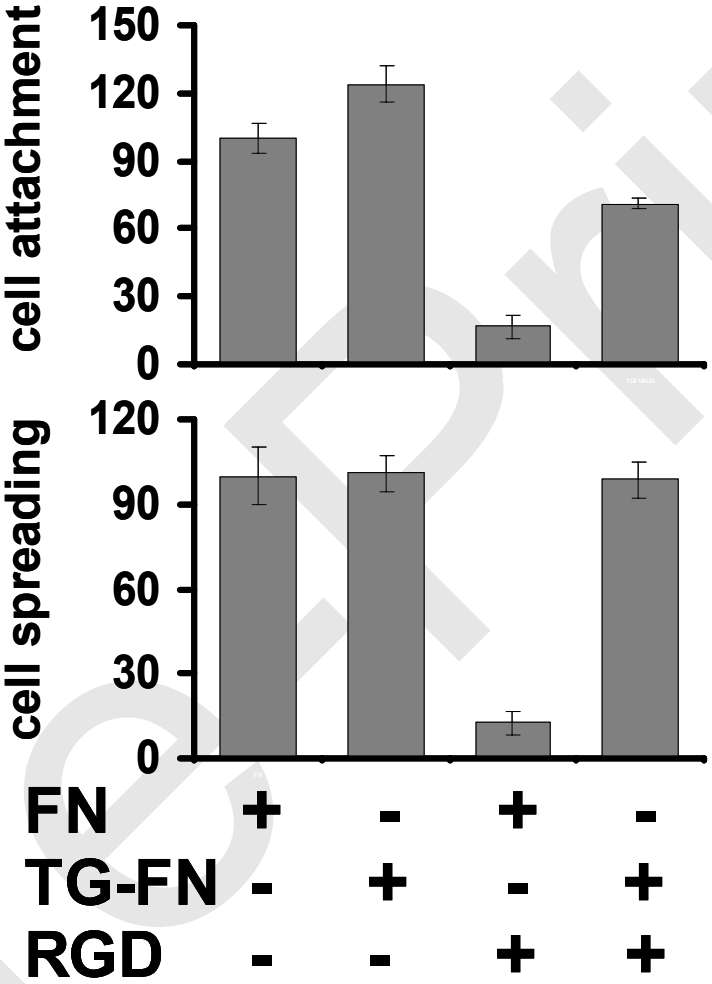

Cell attachment (upper graph) and cell spreading (lower graph) on FN and tTG-FN was assessed in cells pre-incubated with RGD peptide (100 μg/ml) where indicated, as described in legend to Fig. 1, but 4h after seeding cells on FN or tTG-FN. Data were acquired and expressed as percentage of control value on FN as described in legend to Fig. 1 and represent one of two typical experiments, each undertaken in quadruplicate. Mean attachment values ±SD on FN control were 400±27; mean percentage values of spread cells on FN control were 87±9. Total cells analysed in control were ~1600.